

## A critical re-examination and a revised phase diagram of $\text{La}_{1-x}\text{Sr}_x\text{CoO}_3$

To cite this article: D Samal and P S Anil Kumar 2011 *J. Phys.: Condens. Matter* **23** 016001

View the [article online](#) for updates and enhancements.

### You may also like

- [Distribution of Water Pollution SubBengawan Solo Upstream Watershed on Central Java in 2020](#)  
Nanda Regita Cahyaning Putri, Ifan Deffinika and Dicky Arinta
- [Isospin Momentum-Dependent Interaction and Its Role on the Isospin Fractionation Ratio in Intermediate Energy Heavy Ion Collisions](#)  
Liu Jian-Ye, Guo Wen-Jun, Xing Yong-Zhong et al.
- [Effects of Velocity-Dependent Force on the Magnetic Form Factors of Odd-Z Nuclei](#)  
Dong Tie-Kuang and Ren Zhong-Zhou

# A critical re-examination and a revised phase diagram of $\text{La}_{1-x}\text{Sr}_x\text{CoO}_3$

D Samal<sup>1</sup> and P S Anil Kumar

Department of Physics, Indian Institute of Science, Bangalore 560012, India

E-mail: [debphy@physics.iisc.ernet.in](mailto:debphy@physics.iisc.ernet.in) and [anil@physics.iisc.ernet.in](mailto:anil@physics.iisc.ernet.in)

Received 27 May 2010, in final form 7 November 2010

Published 6 December 2010

Online at [stacks.iop.org/JPhysCM/23/016001](http://stacks.iop.org/JPhysCM/23/016001)

## Abstract

We report the results of a comprehensive study on dc magnetization, ac susceptibility, and the magnetotransport properties of the  $\text{La}_{1-x}\text{Sr}_x\text{CoO}_3$  ( $0 \leq x \leq 0.5$ ) system. At higher Sr doping ( $x \geq 0.18$ ), the system exhibits Brillouin-like field cooled magnetization ( $M_{\text{FC}}$ ). However, for  $x < 0.18$ , the system exhibits a kink in the  $M_{\text{FC}}$ , a peak at the intermediate field in the thermoremanent magnetization and a non-saturating tendency in the  $M-H$  plot that all point towards the characteristic of spin glass behavior. More interestingly, dc magnetization studies for  $x < 0.18$  do not suggest the existence of ferromagnetic correlation that can give rise to an irreversible line in the spin glass regime. The ac susceptibility study for  $x > 0.2$  exhibits apparently no frequency dependent peak shift around the ferromagnetic transition region. However, a feeble signature of glassiness is verified by studying the frequency dependent shoulder position in  $\chi''(T)$  and the memory effect below the Curie temperature. But, for  $x < 0.18$ , the ac susceptibility study exhibits a considerable frequency dependent peak shift, time dependent memory effect, and the characteristic spin relaxation time scale  $\tau_o \sim 10^{-13}$  s. The reciprocal susceptibility versus temperature plot adheres to Curie–Weiss behavior and does not provide any signature of preformed ferromagnetic clusters well above the Curie temperature. The magnetotransport study reveals a cross over from metallic to semiconducting-like behavior for  $x \leq 0.18$ . On the semiconducting side, the system exhibits a large value of magnetoresistance (upto 75%) towards low temperature and it is strongly connected to the spin dependent part of the random potential distribution in the spin glass phase. Based on the above observations, we have reconstructed a new magnetic phase diagram and characterized each phase with associated properties.

(Some figures in this article are in colour only in the electronic version)

## 1. Introduction

Extensive studies on transition metal perovskites such as manganites, cobaltites and cuprates over recent decades have revolutionized the understanding of the electronic correlation effect. The most remarkable properties such as metal–insulator transition, colossal magnetoresistance (CMR) in manganites and high  $T_c$  superconductivity in cuprates have spurred enough excitement to carry forward further research in this direction in order to understand the genesis of such unique properties. In a general view, the simultaneous existence of strong electron–electron interaction ( $U$ ) within the transition metal ion and a sizable hopping ( $t_{ij}$ ) between

transition metal 3d and oxygen 2p states are primarily responsible for such a wide range of magnetic and transport properties. Although, the cobaltites do not exhibit CMR effects unlike manganites, the unique temperature induced spin state transition (SST) and a rich variety of magnetic and transport properties have attracted considerable interest. In particular, the hole doped  $\text{La}_{1-x}\text{Sr}_x\text{CoO}_3$  compounds have attracted great attention during the last few decades because of their novel magnetic and electrical transport properties [1–10] and a complicated magnetic ( $x-T$ ) phase diagram [11–13]. The rhombohedrally distorted parent compound  $\text{LaCoO}_3$  at low temperature behaves like a charge transfer type nonmagnetic insulator in which a charge gap is formed between the occupied oxygen 2p band and the 3d  $e_g$  band [14, 15]. However, it

<sup>1</sup> Author to whom any correspondence should be addressed.

can undergo a thermally induced SST from the low spin (LS) state ( $t_{2g}^6 e_g^0$ ;  $S = 0$ , nonmagnetic) to the intermediate spin (IS) state ( $t_{2g}^5 e_g^1$ ;  $S = 1$ ) or the high spin (HS) state ( $t_{2g}^4 e_g^2$ ;  $S = 2$ ) with an increase in temperature and moreover it also exhibits a transition from semiconducting to metallic behavior above  $\sim 500$  K [16–21]. The extra degree of freedom in the ‘spin state’ at the Co site in addition to the lattice, charge and spin degrees of freedom found in some other transition metal oxides has made it more fascinating. The SST in cobaltites is favorable due to comparable sizes ( $\sim 10$  meV) of the crystal field energy ( $\Delta_{cf}$ ) and Hund’s exchange energy ( $\Delta_{ex}$ ). However, the spin density functional band structure calculation on  $\text{La}_{1-x}\text{Sr}_x\text{CoO}_3$  by Ravindran *et al* [5] suggested that the hole doping only stabilizes the IS state as observed experimentally [12] and moreover they also showed that the HS state cannot be stabilized by the temperature or hole doping since the HS state is significantly higher in energy than the LS or IS state.

Earlier studies on  $\text{La}_{1-x}\text{Sr}_x\text{CoO}_3$  report that the system can evolve from semiconducting spin glass (SG) to metallic ferromagnetic (F) behavior with an increase in Sr doping concentration [11, 22]. However, the boundary between the two phases and even the exact characteristic of each phase is not understood even today. It is observed that the higher doping samples not only exhibit the characteristic of long range F order but also manifest the existence of glassy behavior [23, 24]. Similarly, the low doping samples ( $x < 0.18$ ) not only exhibit the characteristic of SG behavior, but also show an irreversibility temperature ( $T_{irr}$ ) [12, 25, 26] indicating a strong F correlation in the SG regime. However, the recent work by Samal *et al* [27, 28] on polycrystalline  $\text{La}_{0.85}\text{Sr}_{0.15}\text{CoO}_3$  could not observe such an existence of  $T_{irr}$  arising out of F correlation.

In spite of continuing studies, many fundamental problems such as glassy behavior (canonical SG or cluster glass), spin states of Co ions and the effect of the SG state on magnetic and transport properties are not well settled yet. Moreover, the hole doped cobaltites such as  $\text{La}_{1-x}\text{Sr}_x\text{CoO}_3$  in single crystalline as well polycrystalline forms have been reported to exhibit electronic/magnetic phase separation (PS) over the past few years. This has enormously triggered renewed interest in the doped cobaltite system. Various experimental techniques such as NMR [29, 30], neutron diffraction [31], magnetic and resistivity relaxation [24, 32], etc reveal the phase segregation in this system. The presence of an irreversibility line along with the preformation of ferromagnetically ordered clusters [12, 13] well above the true long range F ordering temperature is widely observed in the ( $x$ - $T$ ) phase diagram of  $\text{La}_{1-x}\text{Sr}_x\text{CoO}_3$  and it is solely attributed to the PS scenario.

In order to understand the complexity of the true magnetic ground state of the  $\text{La}_{1-x}\text{Sr}_x\text{CoO}_3$  system, we have undertaken an elaborate magnetic and magnetotransport study of eight compositions in the range  $0 \leq x \leq 0.5$ . Based on our present experimental findings, we have reconstructed a magnetic phase diagram by characterizing each phase with the associated properties.

## 2. Sample preparation and experimental details

Polycrystalline  $\text{La}_{1-x}\text{Sr}_x\text{CoO}_3$  ( $0 < x < 0.5$ ) samples are synthesized by a conventional solid state reaction method using a stoichiometric mixture of  $\text{La}_2\text{O}_3$  (preheated at  $800^\circ\text{C}$ ),  $\text{Co}_3\text{O}_4$  and  $\text{SrCO}_3$  precursors. At first, the mixture is calcined at  $900^\circ\text{C}$  in air with several intermediate grindings for homogenization and to form the single phase. Then the calcined mixture is further annealed at  $1300^\circ\text{C}$  with several intermediate grindings followed by the final grinding before the powder is pressed into pellets. The pellets were then sintered at  $1300^\circ\text{C}$  for 24 h and then slowly cooled down to room temperature. The x-ray diffraction measurements were performed at various steps of the preparation to monitor the progress of the phase formation and eventually the compound was found to be single phase as reported earlier [27]. Most of the dc magnetization measurements are performed using a Quantum Design superconducting quantum interference device (SQUID) magnetometer in the temperature range of 10–300 K and a magnetic field up to 5 T. The high temperature dc magnetization measurements are carried out using a commercial vibrating sample magnetometer (VSM) in the temperature range from  $\sim 300$  to 450 K. Ac susceptibility measurements are performed by a commercial Cryobind system down to a temperature of 4.2 K in the frequency range from 15 Hz to 1 KHz. The electrical and magnetotransport properties are measured using a standard four probe van der Pauw configuration in a magnetic field up to 11 T. Silver-indium contacts were employed to give four probe connections to all the samples. All the magnetotransport studies are carried out with a configuration in which the current direction is perpendicular to the applied field direction.

## 3. Results and discussion

### 3.1. Dc magnetization

Figure 1 displays the temperature dependent dc magnetization for seven samples, namely  $x = 0.5, 0.4, 0.3, 0.2, 0.18, 0.15$ , and 0.1. Both the field cooled (FC) and zero field cooled (ZFC) measurements performed at 100 Oe are presented. The field cooled magnetization ( $M_{FC}$ ) curves for  $0.18 \leq x \leq 0.5$  exhibit Brillouin-like behavior which signifies the typical characteristic for F materials. In contrast, as  $x$  gradually reduces to 0.15 and 0.1, the  $M_{FC}$  curves no longer exhibit Brillouin-like behavior, rather they exhibit the characteristic of SG behavior. It is observed that the  $M_{FC}$  curve for  $x = 0.15$  exhibits a kink below the freezing temperature ( $T_f$ ) i.e.  $\sim 60$  K and for  $x = 0.1$  it remains almost flat below  $T_f$  ( $\sim 37$  K). Moreover, the magnetization at low temperature for  $x = 0.1$  and 0.15 is found to be very much less as compared to other ( $x \geq 0.18$ ) compositions. The  $M_{ZFC}$  curves for  $x = 0.1$  and 0.15 decrease very rapidly below the corresponding  $T_f$ s, and as a result they exhibit cusp-like behavior indicating the formation of an SG state.

It has to be noted here that there are many reports [12, 25, 26] from different groups which show a bifurcation between the ZFC and FC curves for  $x < 0.18$  to occur at the irreversibility temperature ( $T_{irr}$ ) and generally  $T_{irr} \gg$

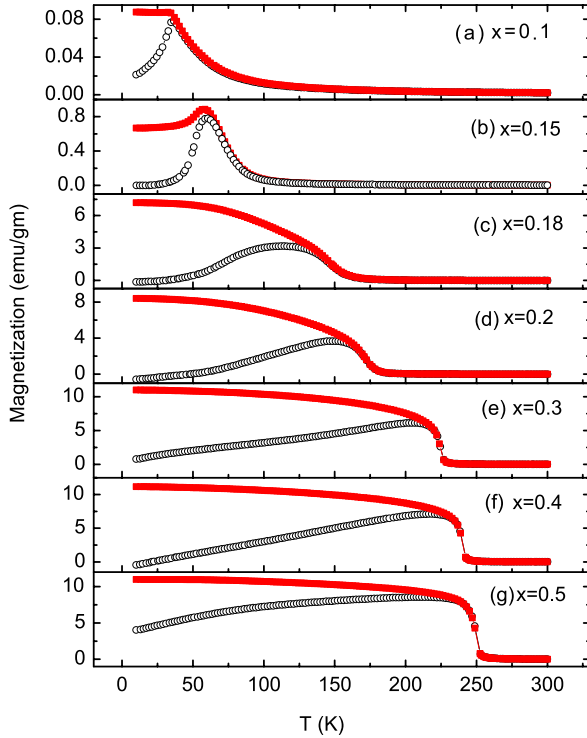


**Figure 1.** The temperature dependence of the FC and ZFC dc magnetizations for  $x = 0.1$  (a),  $0.15$  (b),  $0.18$  (c),  $0.2$  (d),  $0.3$  (e),  $0.4$  (f), and  $0.5$  (g) at  $100$  Oe. The FC curves are shown as solid symbols, whereas the ZFC curves are shown as open symbols.

$T_f$ . Various models such as microscopic magnetic PS and superparamagnetic clusters based on magnetic inhomogeneous states have been proposed to explain such behavior. But it is interesting to observe from our data ( $x = 0.15, 0.1$ ) that the bifurcation between ZFC and FC starts to appear exactly at  $T_f$  or very close to  $T_f$  and no such  $T_{\text{irr}}$  originating from microscopic magnetic PS or F ordering is found above  $T_f$ . Thus the dc magnetization data for  $x = 0.1$  and  $0.15$  are consistent with the characteristic of the canonical SG system. Our recent investigation on  $\text{La}_{0.85}\text{Sr}_{0.15}\text{CoO}_3$  [27, 28] has revealed that the most probable ground state for this compound is SG and it hardly inherits any characteristics that arise out of magnetic PS. However, one can prepare a phase separated compound with different magnetic phases but with a single crystallographic phase for the same composition depending on the heat treatment condition and this has been rigorously discussed in [27].

In figure 2 we show the  $M$ - $H$  plots at  $10$  K for six samples with  $0.1 \leq x \leq 0.5$  up to a magnetic field of  $5$  T. For  $x = 0.5, 0.4, 0.3$ , and  $0.2$ ,  $M$  is found to increase sharply with the increasing field and saturation-like behavior appears above  $\sim 2$  T. We also observe that the hysteresis loops are very narrow. However, a careful inspection finds that a small non-saturating component appears to be superimposed on the saturating F component and thus prevents the magnetization from being in a fully saturated state even at a larger applied magnetic field. This is consistent with the cluster model where it was suggested that a non-F matrix of  $\text{Co}^{3+}$  spin with AF interaction exists [12]. A convincingly simple method can

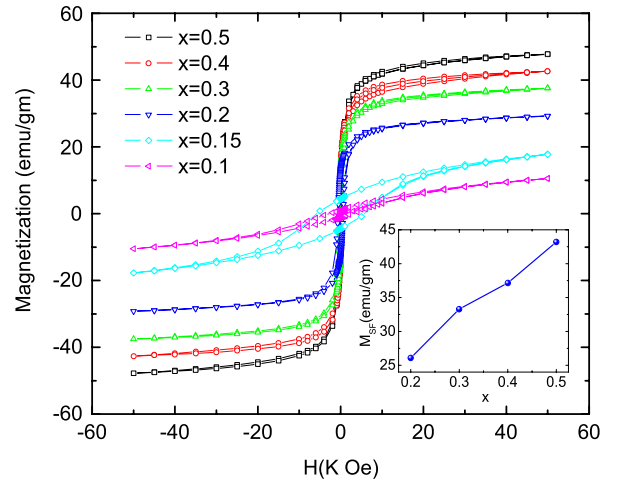


**Figure 2.** The  $M$ - $H$  hysteresis loops at  $10$  K. The inset shows the saturation magnetic moment for the ferromagnetic component ( $M_{\text{SF}}$ ) in  $\text{emu g}^{-1}$  at  $10$  K.

be adopted to separate out the F component from the non-F component arising out of the AF interaction. According to this method, the total high field magnetization is given by  $M_{\text{tot}} = M_{\text{F}} + \chi_{\text{AF}}H$ , where  $M_{\text{F}}$  is the F component and  $\chi_{\text{AF}}$  is the slope of  $M$  versus  $H$  at high field. An extrapolation of this high field behavior back to  $H = 0$  provides the saturated ferromagnetic ( $M_{\text{SF}}$ ) component only. The inset in figure 2 shows the value of saturation  $M_{\text{SF}}$  determined from the  $M$ - $H$  curve using the extrapolation approximation and it is found that the value of  $M_{\text{SF}}$  increases with an increase in  $x$ . The spin state of the Co ion can be determined using the  $M_{\text{SF}}$  in the F phase. The saturation value of magnetization is found to be  $1.7, 1.5, 1.37$  and  $1.1 \mu_{\text{B}}/\text{Co}$  for  $x = 0.5, 0.4, 0.3$ , and  $x = 0.2$  respectively. However, it is realized that the experimentally observed moments are found to be much smaller than the expected spin only moment ( $\mu = gS\mu_{\text{B}}$ , i.e.  $2.5$  ( $x = 0.5$ ),  $2.4$  ( $x = 0.4$ ),  $2.3$  ( $x = 0.3$ ) and  $2.2$  ( $x = 0.2$ )  $\mu_{\text{B}}/\text{Co}$ ) when both  $\text{Co}^{3+}$  ( $S = 1$ ) and  $\text{Co}^{4+}$  ( $S = 3/2$ ) are in the IS. It has to be noted here that the theoretical work by Ravindra *et al* [5] using band structure calculations has suggested that the hole doping in  $\text{La}_{1-x}\text{Sr}_x\text{CoO}_3$  reduces the ionic character, enhances the hybridization between Co and O and uniformly affects the spin state for  $\text{Co}^{3+}$  and  $\text{Co}^{4+}$ . Due to the Co-O hybridization, the expected average Co moment is reduced significantly compared to the simple ionic model.

But on the other hand, one can easily notice from figure 2 that the  $H$  dependence of  $M$  for  $x = 0.15$  and  $0.1$  is very different from that of the other compositions. In the case of  $x = 0.1$  and  $0.15$ ,  $M$  increases steadily with  $H$  without showing any sign of saturation-like behavior up to the highest applied magnetic field. The small value and the lack of saturation of the magnetization for  $x = 0.1$  and  $0.15$  even at relatively higher fields indicate the characteristics of typical SG behavior [11, 33]. In order to further elucidate the existence of SG behavior for  $x < 0.18$ , we have performed measurements for thermoremanent magnetization (TRM) versus  $H$  at  $10$  K in the field range of  $0.01 \text{ T} \leq H \leq 5 \text{ T}$ . To measure the TRM, the system was cooled in the specified field from room

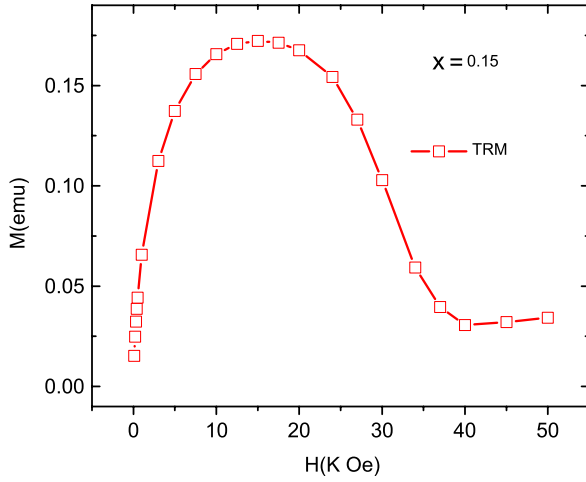


**Figure 3.** Thermoremanent magnetization (TRM) versus  $H$  for  $\text{La}_{0.85}\text{Sr}_{0.15}\text{CoO}_3$  at 10 K.

temperature down to 10 K and subsequently the field was removed, and then magnetization was recorded. For a typical canonical SG system the TRM curve exhibits a characteristic peak at intermediate fields and then tends to saturate at higher fields [34, 35]. Figure 3 shows the TRM curve as a function of applied magnetic field for  $x = 0.15$  and it is evident that the TRM curve qualitatively exhibits very similar behavior to that expected for the canonical SG system.

### 3.2. Ac susceptibility

In figure 4, we show the ZFC in-phase  $\chi'(T)$  (a) and out-of-phase  $\chi''(T)$  (b) components for  $x = 0.5$  measured at various frequencies and in a probing field  $H_{ac} = 170$  mOe. It is observed that at around 250 K both  $\chi'(T)$  and  $\chi''(T)$  abruptly fall to zero and the peak positions are nearly independent of measuring frequency. The frequency, independent of peak position along with the cusp in  $M_{zfc}$ , convincingly indicates a ferromagnetic to paramagnetic phase transition. However, as we go down in temperature, an extra hump-like feature is noticed in  $\chi''(T)$  at  $\sim 185$  K. The inset in figure 4(b) shows the zoomed in view of the hump positions at different frequencies. It is noticed that the position of the hump apparently shifts to higher temperature with an increase in frequency, suggesting a signature of glassy behavior. In order to verify the existence of glassy behavior more clearly, we have carried out the study of the memory effect [24, 36, 37] well below the F ordering temperature. This effect can be illustrated by measuring  $\chi_{ac}$  in two different ways: one by a halting measurement ( $\chi_{halt}$ ) and the other by a reference ( $\chi_{ref}$ ) one. In the halting measurement, the sample was first zero field cooled from room temperature to the lowest temperature with an intermediate halt ( $t_{halt}$ ) of about  $\sim 10$  h at the halting temperature ( $T_{halt}$ ), where  $T_{halt}$  is lower than the corresponding magnetic ordering temperature. Then the magnetic response ( $\chi_{halt}$ ) was recorded during the heating run by applying a probing ac field ( $H_{ac}$ ). However, in the reference measurement, the sample was zero field cooled again from room temperature to the lowest possible temperature without any intermediate halt and regular ZFC

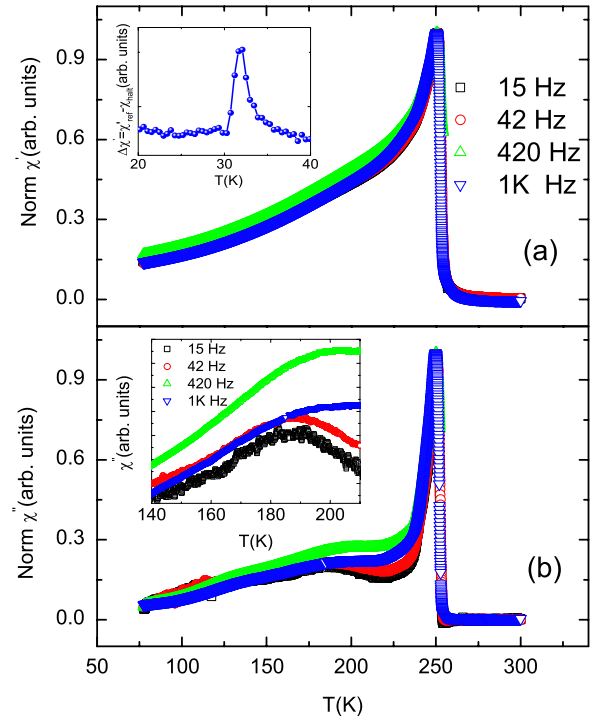


**Figure 4.** The temperature dependence of the ZFC in-phase (a) and out-of-phase (b) ac susceptibility components for  $x = 0.5$ . The inset shows the  $\Delta\chi' = (\chi'_{ref} - \chi'_{halt})$  versus  $T$  around  $T_{halt}$  (a) and the close-ups of the shoulder position with respect to the measuring frequencies (b).

data ( $\chi_{ref}$ ) were recorded during the heating run with the same applied probing  $H_{ac}$ . To demonstrate the memory effect more efficiently, we plot  $\Delta\chi = (\chi_{ref} - \chi_{halt})$  versus  $T$  and the observed peak in  $\Delta\chi$  around the  $T_{halt}$  reflects the memory effect indicating glassy behavior. The inset in figure 4(a) shows  $\Delta\chi' = (\chi'_{ref} - \chi'_{halt})$  versus  $T$  exhibiting a peak around  $T_{halt}$  (i.e. 30 K) that reflects the memory effect. In essence, the ac susceptibility results on  $\text{La}_{0.5}\text{Sr}_{0.5}\text{CoO}_3$  suggest the coexistence of both ferromagnetism and glassy behavior. Very similar to  $x = 0.5$ , the ac susceptibility study on  $x = 0.4$  and  $0.3$  also exhibits a feeble shoulder-like feature in  $\chi''(T)$  below the F ordering. However, the frequency dependence of the shoulder position is less pronounced unlike what is observed for  $x = 0.5$ . The frequency dependent hump shift and the memory effect truly indicate that even in the F regime of the  $\text{La}_{1-x}\text{Sr}_x\text{CoO}_3$  system, the system does not possess conventional long range F ordering. Rather, it possesses F clusters which are responsible for the ‘Brillouin-like’ temperature dependent FC magnetizations and probably the interactions among them could lead to glassy behavior. In fact, the work by Tang *et al* [24] on  $\text{La}_{0.82}\text{Sr}_{0.18}\text{CoO}_3$  suggested that both intercluster interaction and the SG-like phase can contribute to glassy magnetic behavior.

Figures 5(a) and (b) display normalized ZFC  $\chi'(T)$  at various frequencies in a probing field  $H_{ac} = 170$  mOe, for  $x = 0.1$  and  $x = 0.15$  respectively. It is observed that both the samples exhibit a pronounced frequency dependent peak shift to higher temperature with increasing frequencies. The insets in figures 5(a) and (b) clearly show the close up views of

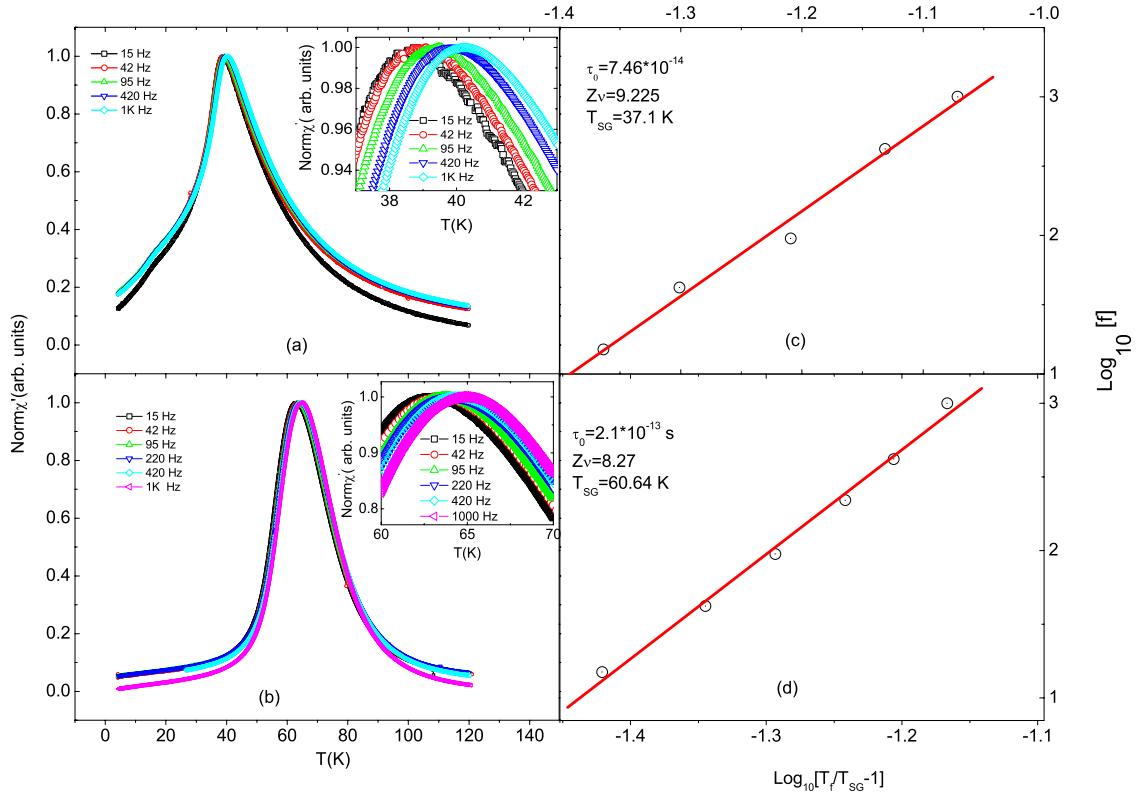


**Figure 5.** The temperature dependence of the ZFC in-phase ac susceptibility for  $x = 0.1$  (a) and  $0.15$  (b) at various measuring frequencies as indicated in the figure. The insets in (a) and (b) show the close-ups of the peak position with respect to the measuring frequencies. We show plots of  $\log_{10} f$  versus  $\log_{10}[(T_f/T_{SG}) - 1]$  for  $x = 0.1$  (c) and  $x = 0.15$  (d) in accordance with the equation for ‘critical slowing down’ of the spin dynamics. The dashed lines represent the best fit to the data with the fitting parameters as shown in the figure.

the peak positions with increasing measuring frequency. The frequency dependent peak shifts in  $\chi'(T)$  can be quantified, i.e.  $s = \Delta T_f / T_f \Delta \log_{10} f = 0.021$  and  $0.016$  for  $x = 0.1$  and  $x = 0.15$  respectively, where  $\Delta T_f = (T_{f1} - T_{f2})$ ,  $\Delta \log_{10} f = (\log_{10} f_1 - \log_{10} f_2)$  with  $f_1 = 1000$  Hz and  $f_2 = 15$  Hz. The estimated values are typical for the canonical SG where ‘ $s$ ’ ranges from  $0.0045$  to  $0.08$  [38]. Moreover, the dependence of  $T_f$  on  $f$  can be well described by the conventional ‘critical slowing down’ of the spin dynamics. In the language of SG, it can be written as  $\tau = \tau_0 (T/T_{SG} - 1)^{-z\nu}$  [12, 39–41] where  $T_{SG}$  is the critical temperature for SG ordering (i.e.  $T_{SG} = T_f$  when  $f \rightarrow 0$ ),  $z\nu$  is a constant exponent,  $\tau_0$  is the characteristic time scale for the spin dynamics, and  $T_f$  is the frequency dependent freezing temperature. The agreement with the above equation is validated by plotting  $\log_{10}(f)$  versus  $\log_{10}[(T_f/T_{SG}) - 1]$  in figures 5(c) and (d) for  $x = 0.1$  and  $x = 0.15$  respectively. To obtain the best fit for the equation representing the ‘critical slowing down’ process,  $T_{SG}$  is adjusted such that the least-square deviation in a straight line fit is minimum. The best fits are found to occur at  $T_{SG} \sim 37.1$  and  $60.6$  K for  $x = 0.1$  and  $x = 0.15$  respectively. The values of  $\tau_0$  and  $z\nu$  are obtained as  $\tau_0 = 7.46 \times 10^{-14}$  s,  $z\nu = 9.23$  and  $\tau_0 = 2.1 \times 10^{-13}$  s,  $z\nu = 8.27$  for  $x = 0.1$  and  $x = 0.15$  respectively from the intercept and the slope of the straight lines. It is encouraging to note that the values obtained for  $z\nu$  and  $\tau_0$  are comparable to those reported for typical canonical SG systems [39]. It has to

be pointed out here that the value of  $T_{SG}$  derived from ‘critical slowing down’ of the spin dynamics agrees well with the value obtained by a simple extrapolation of  $T_f$  when  $f \rightarrow 0$ .

### 3.3. Memory effect for $x = 0.15$ and $0.1$

Due to the slow dynamics associated with the SG state, it does not reach the equilibrium state within the experimental time scale. This as a result leads to nonequilibrium phenomena such as memory and ageing effects. Figures 6(a) and (b) show the memory effects studied for  $x = 0.1$  and  $x = 0.15$  at  $T_{\text{halt}} = 20$  K and  $30$  K respectively using the same protocol as described above. The  $T_{\text{halt}}$  s in both the cases are below the corresponding  $T_f$  s. In figure 6, we show a clear distinction between  $\chi'_{\text{ref}}$  and  $\chi'_{\text{halt}}$  for both the samples around the corresponding  $T_{\text{halt}}$ . Moreover, the insets in figure 6 exhibit pronounced peaks in  $\Delta\chi'$  versus  $T$  around the corresponding  $T_{\text{halt}}$  and characterize the system to be glassy in nature. It has to be mentioned here that the work by Sasaki *et al* [42] suggested that the ageing and memory effects are not sufficient proof for the existence of SG dynamics. However, the frequency dependent variation of  $T_f$ , reduced value of low temperature  $M_{FC}$ , non-saturating tendency of the  $M-H$  plot even at a relatively high applied field, the memory effect, and the relaxation time  $\tau_0$  ( $\sim 10^{-13}$  s) all rolled together characterize both ( $x = 0.1$  and  $0.15$ ) the systems to be SG in origin.

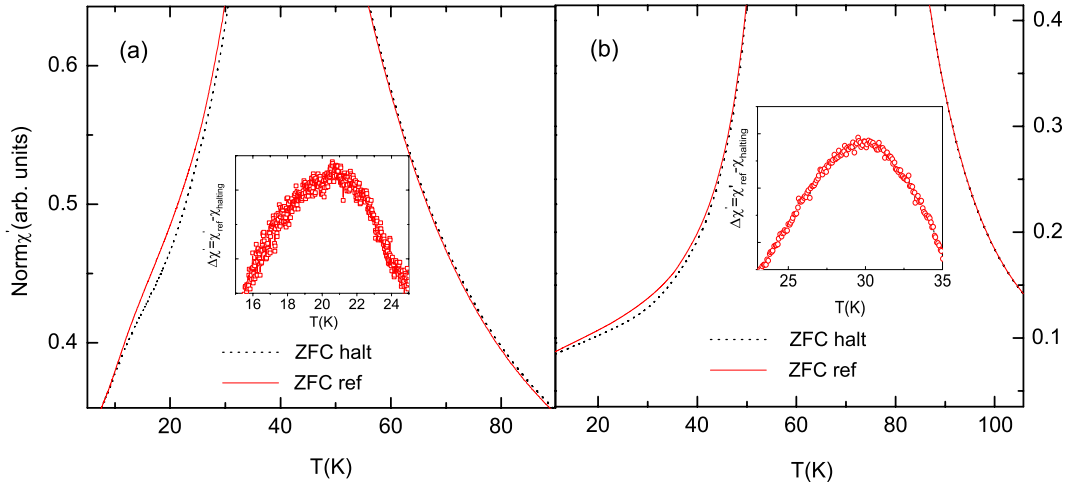


**Figure 6.** The temperature dependence of the ZFC in-phase ac susceptibility  $\chi'_{ref}$  and the  $\chi'_{halt}$  for  $x = 0.1$  (a) and  $x = 0.15$  (b). The insets show the  $\Delta\chi' = (\chi'_{ref} - \chi'_{halt})$  versus  $T$  around the  $T_{halt}$ .

### 3.4. Spin state determination from the paramagnetic susceptibility

In order to examine the spin state of Co ions in the paramagnetic state, we have performed high temperature VSM experiments from  $\sim 310$  to 440 K. In the paramagnetic phase the spin state can be extracted from the Curie–Weiss (CW) law,

$$\chi = \frac{C}{T - \theta}, \quad \text{where } C = \frac{N\mu_{eff}^2}{3k_B} \quad \text{and} \\ \mu_{eff} = g[S(S + 1)]^{1/2}\mu_B.$$

Here,  $\chi$  is the susceptibility,  $C$  is the Curie constant,  $N$  is the number of Co ions per gram,  $\mu_{eff}$  is the effective number of the Bohr magneton and  $g$  is the Lande  $g$  factor. It is always useful to collect data over a wide range of temperature since it can shed light about a high temperature structural transition that can influence the effective moments. Unfortunately, we are not able to investigate the temperature dependence of the paramagnetic effective moment over a wide range of temperature due to the experimental constraints and thus provide a rough estimation of it from the narrow range of our measurement. Figure 7 plots the reciprocal susceptibility ( $\chi^{-1}$ ) as a function of temperature for  $x = 0.5$  and 0.3. It is seen from figure 7 that the curves fit reasonably well to a straight line and the slope of the fitted curve provides the average spin value ( $S_{avg}$ ) and the intercept yields  $\theta$ , where  $S_{avg} = (1 - x)Co^{3+} + xCo^{4+}$ . The value of  $S_{avg}$  is found to be 1.35 and 1.31 for  $x = 0.5$  and 0.3 respectively. According to the ionic model, the situation where  $Co^{3+}$  are in IS state ( $S = 1$ ) and  $Co^{4+}$  are also in IS state ( $S = 3/2$ ) results in the  $S_{avg}$  being 1.25 and 1.15 for  $x = 0.5$  and  $x = 0.3$  respectively. Indeed the rough estimated value of  $S_{avg}$  from our data is in good agreement with the IS configuration of Co spins. However, it has to be noted here that the magnetic moment ( $\mu_B/Co$ ) determined from the low temperature saturation moment differs greatly in magnitude as compared to the values obtained from paramagnetic susceptibility study. To make a simple comparison, the values of magnetic moment

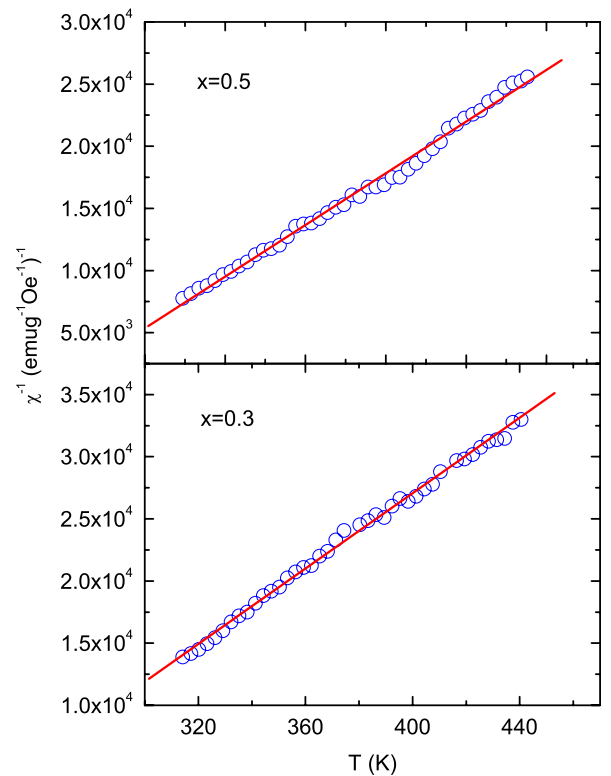


**Figure 7.** The temperature dependence of reciprocal susceptibility ( $\chi^{-1}$ ) for  $x = 0.5$  (a) and  $x = 0.3$  (b) above the magnetic transition temperatures. Solid lines show the Curie–Weiss linear fit to the data obtained from VSM measurements.

estimated from paramagnetic and low temperature saturated magnetization study are found to be 2.7 and 1.7  $\mu_B/Co$  for  $x = 0.5$ , 2.6 and 1.37  $\mu_B/Co$  for  $x = 0.3$  respectively. The reduced value of magnetic moment ( $\mu_B/Co$ ) obtained from the low temperature saturation magnetic moment analysis directly hints at the existence of a non-F matrix with AF interaction in the ordered state. However, as the temperature rises above the Curie temperature, then all the cooperative

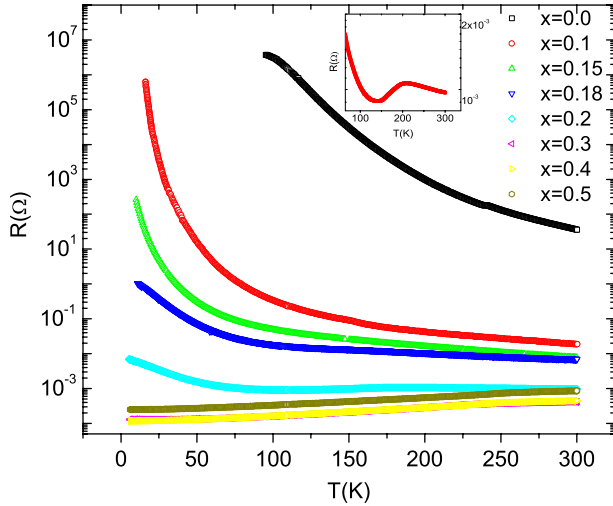


**Figure 8.** The temperature dependent resistance of  $\text{La}_{1-x}\text{Sr}_x\text{CoO}_3$  for  $0.0 \leq x \leq 0.5$ . The inset shows the zoomed in view of the resistance versus temperature curve for  $x = 0.2$ .

ordering phenomena die away and we get the magnetic moment ( $\mu_B/\text{Co}$ ) very close to what is expected from the ionic model.

More interestingly, it has to be pointed out here that the recent work by Leighton *et al* [13] on the  $\text{La}_{1-x}\text{Sr}_x\text{CoO}_3$  system observed an upward deviation from the CW plot at  $T \gg T_c$  ( $\sim 360$  K) and it was interpreted as the possible existence of preformed F clusters well above  $T_c$ . However, our experimental data for  $x = 0.5$  and  $0.3$  do not exhibit any such upward deviation from CW behavior and thus in turn suggest no such possible existence of preformed F clusters well above the Curie temperature. Thus, within the domain of our experiments, the experimental finding reveals (i) the existence of an intermediate spin state of Co ions in the paramagnetic state and (ii) no possible existence of preformed ferromagnetic clusters well above the Curie temperature.

### 3.5. Magnetotransport

Figure 8 plots the resistance ( $R$ ) versus temperature ( $T$ ) curves that show an evolution from semiconducting-like behavior to metallic behavior with an increase in  $x$ . It is observed that for  $x = 0.0, 0.1, 0.15$  and  $0.18$ , the samples exhibit semiconducting-like ( $dR/dT < 0$ ) behavior whereas for  $x = 0.3, 0.4$ , and  $0.5$  the samples show the characteristic of metallic ( $dR/dT > 0$ ) behavior. However  $R$ - $T$  behavior for the  $x = 0.2$  sample exhibits an interesting feature by changing the slope ( $dR/dT$ ) at various temperatures. It is observed that in the window of  $\sim 200$ – $140$  K,  $dR/dT > 0$  indicating metallic behavior. But on the other hand, as we move towards the lower temperature side (i.e. below  $140$  K),  $dR/dT < 0$  and it indicates a semiconducting behavior as shown in the inset of figure 8. This can be understood as a re-entrant insulator–metal transition as suggested by Senaris Rodriguez *et al* [1]. It has to be remembered here that a very similar kind of result has also been observed by Kundu *et al* [36] in glassy  $\text{La}_{0.7}\text{Ca}_{0.3}\text{CoO}_3$  single crystalline samples. Moreover, it is also noticed that

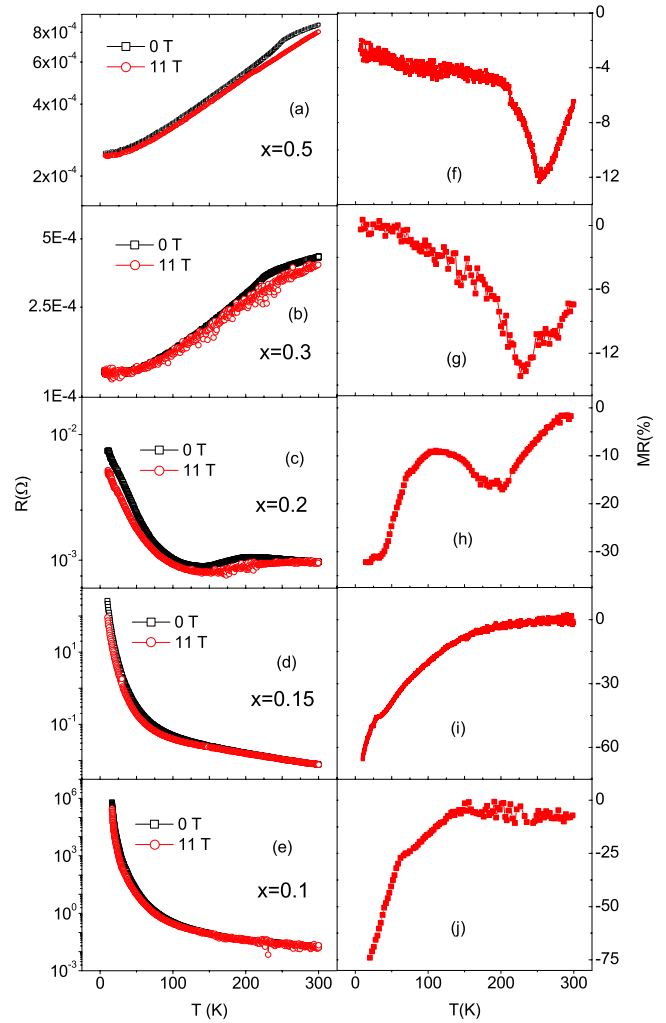


**Figure 9.** The temperature dependent resistance for  $x = 0.5$  (a),  $0.3$  (b),  $0.2$  (c),  $0.15$  (d) and  $0.1$  (e) in  $H = 0$  and  $11$  T. The calculated MR as a function of temperature for  $x = 0.5$  (f),  $0.3$  (g),  $0.2$  (h),  $0.15$  (i) and  $0.1$  (j).

$dR/dT$  is negative above  $T_c$  for  $x = 0.2$  and this is in contrast to what has been observed for higher doping ( $x = 0.5, 0.4$ , and  $0.3$ ) F metallic samples. This indicates quite remarkably that the concentration of F clusters and their respective sizes present in the non-F insulating matrix have a strong influence on  $R(T)$  above  $T_c$ .

Further, the magnetoresistance (MR) behavior of the  $\text{La}_{1-x}\text{Sr}_x\text{CoO}_3$  system exhibits fascinating characteristics depending crucially on the level of Sr substitution. Figure 9 shows the temperature dependent MR (i.e.  $[[R(H) - R(0)]/R(0)]$ ) behavior for five representative samples ( $x = 0.5, 0.3, 0.2$  and  $0.15$ , and  $0.1$ ) in the presence of an applied field of  $11$  T. For the higher doping F metallic samples such as  $x = 0.5$  and  $0.3$ , the MR plot exhibits a negative maximum in the vicinity of  $T_c$  and then declines as we go down in temperature. The maximum value of MR% in both the cases is found to be  $12$ – $13\%$  at the corresponding  $T_c$ s. Generally, a maximum in MR could occur around the Curie temperature owing to large spin fluctuation when the ferromagnetism starts to set in and as the temperature decreases, the system improves its magnetic order and the MR decreases sharply. The negative

MR observed in these samples can be qualitatively understood within the framework of the DE model proposed by Zener [43]. However, the predictions of this model are not quantitatively very correct. The later work by Goodenough [44] on  $\text{La}_{1-x}\text{Sr}_x\text{CoO}_3$  proposed that a ferromagnetic  $\text{Co}^{3+}\text{-Co}^{4+}$  interaction could be possible from a modified superexchange consideration. However, the superexchange model is generally applicable to localized electron systems and thus very useful for insulating magnetic systems. It has to be noted here that the recent work by Xie *et al* [45] on  $\text{La}_{0.5}\text{Sr}_{0.5}\text{CoO}_3$  thin films reported that the superexchange interaction might be a better match for the observation of ferromagnetism in this compound.

The MR behavior for  $x = 0.2$  exhibits a distinct feature as shown in figure 9(h). It is observed that the MR exhibits a broad dip around  $T_c$  and then further increases to a higher value in the low temperature semiconducting regime. Further as we move into the SG insulating regime, i.e.  $x = 0.1$  and 0.15, it is found that the MR monotonically increases to a higher value with lowering temperature. The value of MR% at low temperature for  $x = 0.15$  as shown in figure 9 is found to be very similar to the high MR% which was observed earlier [27] by performing low temperature  $R\text{-}H$  measurements at different fixed temperatures. The origin of such a huge MR is not unambiguously understood, but is believed to be due to the spin dependent part of the random potential distribution which gets suppressed greatly when the spins get aligned in the presence of the magnetic field [12, 46]. In an SG system, all the spins are frozen in random directions due to different local anisotropies. But upon applying a large magnetic field, the randomness of the spin configuration is suppressed and they tend to align in the direction of the applied magnetic field. This process enhances the hopping probability and thus it leads to a drastic reduction of resistance resulting in such a huge MR. However, it is worth mentioning here is that since our investigation is on polycrystalline samples, it is possible that the spin dependent scattering between grains at the grain boundaries can also influence the transport properties. In essence, the understanding of magnetotransport behavior of polycrystalline samples is a complex issue and it can strongly depend upon the sample microstructure. Moreover, it is interesting to observe from figures 9(i) and (j) that no anomaly in the MR is found near  $T_f$ , which in turn suggests that the spin freezing has apparently no effect either in resistance or MR. The effect of SG freezing on the electrical transport properties is still today an open question and it needs to be understood thoroughly.

Combining all the magnetic (ac and dc) and transport results of our present investigation, we are able to reconstruct a magnetic phase diagram as shown in figure 10. The salient features that have been incorporated in the revised phase diagram are (a) no existence of a  $T_{\text{irr}}$  line in the SG regime (b) no existence of preformed F clusters well above the Curie temperature for higher doping samples and (c) a temperature induced metal–semiconductor transition.

#### 4. Conclusion

We have presented detailed dc magnetization, ac susceptibility and magnetotransport results on polycrystalline

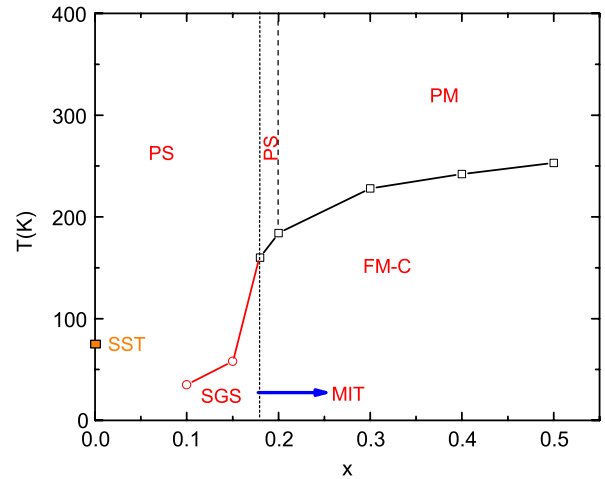


**Figure 10.** Magnetic phase diagram (in the  $x\text{-}T$  plane) for  $\text{La}_{1-x}\text{Sr}_x\text{CoO}_3$ . PM, PS, SGS, FM-C, and MIT abbreviations denote paramagnetic metal, paramagnetic semiconductor, spin glass semiconductor, ferromagnetic metallic-cluster, and metal–insulator transition. The solid square denotes the spin state transition temperature ( $T_{\text{SST}}$ ) for  $x = 0$ .

$\text{La}_{1-x}\text{Sr}_x\text{CoO}_3$  samples of eight various compositions with  $0 \leq x \leq 0.5$ . For  $x \geq 0.18$  the FC curves exhibit Brillouin-like behavior indicating F ordering, however for  $x < 0.18$  they exhibit the characteristic of SG behavior. Most astonishingly, the dc magnetization study does not observe the existence of  $T_{\text{irr}}$  ( $T_{\text{irr}} \gg T_f$ ) which is generally believed to occur due to F correlation present in the SG regime. The ac susceptibility study for  $x < 0.18$  exhibits a pronounced frequency dependent peak shift, time dependent memory effects, and relaxation time  $\tau_o$  ( $\sim 10^{-13}$  s), all of which point towards the characteristic of SG behavior. But for  $x > 0.18$ , it exhibits apparently no frequency dependent peak shift around the F transition region. However, for  $x > 0.18$ , we do observe a trace of glassiness present along with the long range F ordering. The glassiness is characterized both by the memory experiment and the shift of shoulder position in  $\chi''(T)$  with measuring frequency below the F ordering temperature. The spin moment estimated from high temperature magnetization study is in good agreement with the IS configuration of Co ions. The  $\chi^{-1}$  versus  $T$  plot follows strictly the CW law and does not show any indication for the presence of preformed F clusters well above the Curie temperature. The transport study shows an evolution from semiconducting-like behavior to metallic behavior with increase in Sr doping concentration. The metallic samples exhibit a maximum in MR value in the vicinity of the Curie temperature as generally observed in CMR effects. However, the MR plot for semiconducting SG samples exhibits a much higher value (up to 75%) in the low temperature side and decreases monotonically with increase in temperature. Such a high value of MR in the case of semiconducting SG samples is believed to be due to the spin dependent part of the random potential distribution that gets suppressed with the application of magnetic field. Based on all the experimental findings, the magnetic phase diagram has been constructed and the characteristic of each phase has been established.

## Acknowledgment

The authors gratefully acknowledge the use of the National Facility for Low Temperature and High Magnetic Field (LTHMF), Indian Institute of Science (IISc).

## References

- [1] Senaris Rodriguez M A and Goodenough J B 1995 *J. Solid State Chem.* **118** 323
- [2] Caciuffo R, Rinaldi D, Barucca G, Mira J, Rivas J, Senaris Rodriguez M A, Radaelli P G, Fiorani D and Goodenough J B 1999 *Phys. Rev. B* **59** 1068
- [3] Golovanov V, Mihaly L and Moodenbaugh A R 1996 *Phys. Rev. B* **53** 8207
- [4] Ravindran P, Korzhavyi P A, Fjellvag H and Kjekshus A 1999 *Phys. Rev. B* **60** 16423
- [5] Ravindran P, Fjellvag H, Kjekshus A, Blaha P, Schwarz K and Luitz J 2002 *J. Appl. Phys.* **91** 291
- [6] Mukherjee S, Ranganathan R, Anil Kumar P S and Joy P A 1996 *Phys. Rev. B* **54** 9267
- [7] Anil Kumar P S, Joy P A and Date S K 1998 *J. Phys.: Condens. Matter* **10** L487
- [8] Anil Kumar P S, Santhosh P N, Joy P A and Date S K 1998 *J. Mater. Chem.* **8** 2245
- [9] Mandal P, Hassen A and Choudhury P 2006 *J. Appl. Phys.* **100** 103912
- [10] Aarbogh H M, Wu J, Wang L, Zheng H, Mitchell J F and Leighton C 2006 *Phys. Rev. B* **74** 134408
- [11] Itoh M, Natori I, Kubota S and Motoya K 1994 *J. Phys. Soc. Japan* **63** 1486
- [12] Wu J and Leighton C 2003 *Phys. Rev. B* **67** 174408
- [13] He C, Torija M A, Wu J, Lynn J W, Zheng H, Mitchell J F and Leighton C 2007 *Phys. Rev. B* **76** 014401
- [14] Zaanen J, Sawatzky G A and Allen J W 1985 *Phys. Rev. Lett.* **55** 418
- [15] Takahashi H, Munakata and Yamanaka M 1996 *Phys. Rev. B* **53** 3731
- [16] Senaris Rodriguez M A and Goodenough J B 1995 *J. Solid State Chem.* **116** 224
- [17] Korotin M A, Ezhov S Y, Solovyev I V, Anisimov V I, Khomskii D I and Sawatzky G A 1996 *Phys. Rev. B* **54** 5309
- [18] Saitoh T, Mizokawa T, Fujimori A, Abbate M, Takeda Y and Takano M 1997 *Phys. Rev. B* **55** 4257
- [19] Haverkort M W, Hu Z, Cezar J C, Burnus T, Hartmann H, Reuther M, Zobel C, Lorenz T, Tanaka A, Brookes N B, Hsieh H H, Lin H J, Chen C T and Tjeng L H 2006 *Phys. Rev. Lett.* **97** 176405
- [20] Yamaguchi S, Okimoto Y and Tokura Y 1997 *Phys. Rev. B* **55** 8666
- [21] Zobel C, Kriener M, Bruns D, Baier J, Gruninger M, Lorenz T, Reutler P and Revcolevschi A 2002 *Phys. Rev. B* **66** 020402
- [22] Ganguly P, Anil Kumar P S, Santhosh P N and Mulla I S 1994 *J. Phys.: Condens. Matter* **6** 533
- [23] Nam D N H, Jonason K, Nordblad P, Khiem N V and Phuc N H 1999 *Phys. Rev. B* **59** 4189
- [24] Tang Y, Sun Y and Cheng Z 2006 *Phys. Rev. B* **73** 012409
- [25] Yuan S, Xu K, Li Z, Yu L, Kang B and Cao S 2009 *J. Appl. Phys.* **105** 093910
- [26] Phuc N X, Khiem N V and Hoai Nam D N 2002 *J. Magn. Mater.* **242** 754
- [27] Samal D, Shivakumara C and Anil Kumar P S 2009 *J. Appl. Phys.* **106** 123920
- [28] Samal D, Balamurugan K, Shivakumara C and Anil Kumar P S 2009 *J. Appl. Phys.* **105** 07E320
- [29] Hoch M J R, Kuhns P L, Moulton W G and Reys A P 2004 *Phys. Rev. B* **69** 014425
- [30] Kuhns P L, Hoch M J R, Moulton W G, Reys A P, Wu J and Leighton C 2003 *Phys. Rev. Lett.* **91** 127202
- [31] Wu J, Lynn J W, Glinka C J, Burley J, Zheng H, Mitchell J F and Leighton C 2005 *Phys. Rev. Lett.* **94** 037201
- [32] Wu J, Zheng H, Mitchell J F and Leighton C 2006 *Phys. Rev. B* **73** 020404(R)
- [33] Mydeen K, Mandal P, Prabhakaran D and Jin C Q 2009 *Phys. Rev. B* **80** 014421
- [34] Binder K and Young A P 1986 *Rev. Mod. Phys.* **58** 801
- [35] Kinzel W 1979 *Phys. Rev. B* **19** 4595
- [36] Kundu A K, Nordblad P and Rao C N R 2005 *Phys. Rev. B* **72** 144423
- [37] Kundu A K, Nordblad P and Rao C N R 2006 *J. Phys.: Condens. Matter* **18** 4809
- [38] Mydosh J A 1993 *Spin Glasses: An Experimental Introduction* (London: Taylor and Francis) p 67
- [39] Mydosh J A 1993 *Spin Glasses: An Experimental Introduction* (London: Taylor and Francis) p 71
- [40] Gunnarsson K, Svedlindh P, Nordblad P and Lundgren L 1988 *Phys. Rev. Lett.* **61** 754
- [41] Wang F, Kim J and Kim Y J 2009 *Phys. Rev. B* **80** 024419
- [42] Sasaki M, Jonsson P E, Takayama H and Mamiya H 2005 *Phys. Rev. B* **71** 104405
- [43] Zener C 1951 *Phys. Rev.* **82** 403
- [44] Goodenough J B 1958 *J. Phys. Chem. Solids* **6** 287
- [45] Xie C K, Budnick J I, Hines W A, Wells B O and Woicik J C 2008 *Appl. Phys. Lett.* **93** 182507
- [46] Suzanne R, Wu J and Leighton C 2002 *Phys. Rev. B* **65** 220407